Seizure: European Journal of Epilepsy 72 (2019) 54–60

Contents lists available at ScienceDirect

Seizure: European Journal of Epilepsy

journal homepage: www.elsevier.com/locate/seizure

Stereo-EEG ictal/interictal patterns and underlying pathologies

Roberta Di Giacomo[a,b,*,1], Reinaldo Uribe-San-Martin[b,c,1], Roberto Mai[b], Stefano Francione[b], Lino Nobili[b], Ivana Sartori[b], Francesca Gozzo[b], Veronica Pelliccia[b], Marco Onofrj[d], Giorgio Lo Russo[b], Marco de Curtis[a], Laura Tassi[b]

[a] Epilepsy Unit, Fondazione IRCCS Istituto Neurologico Carlo Besta, Via Celoria 11, 20133 Milan, Italy
[b] Claudio MunariEpilepsy Surgery Centre, Niguarda Hospital, Piazza Ospedale Maggiore 3, 20162 Milan, Italy
[c] Neurology Department, Pontificia Universidad Católica de Chile, Neurology Service, Complejo Asistencial Hospital Sótero del Río, Chile
[d] Department of Neuroscience, Imaging and Clinical Sciences, University G. D'Annunzio of Chieti-Pescara, Italy

ARTICLE INFO

Keywords:
Stereo-EEG
Seizure onset zone
Epileptogenic zone
Interictal activity
Malformations of cortical development
Epilepsy surgery

ABSTRACT

Purpose: To define Stereo-EEG (SEEG) ictal and interictal patterns associated with different pathologies in a cohort of patients with drug-resistant focal epilepsy.
Methods: We retrospectively analyzed findings from 102 patient with epilepsy due to Polymicrogyria (PMG), Periventricular Nodular Heterotopia (PNH), Focal Cortical Dysplasia (FCD) type I, IIa, IIb and Hippocampal Sclerosis (HS). Ictal and interictal SEEG recordings were reviewed to describe Seizure Onset Zone (SEEG-SOZ) patterns and to define the Lesional and Irritative Zones.
Results: Five SEEG-SOZ patterns were identified: significant associations were found between low-voltage fast activity and PMG and between repetitive fast spikes bursts and FCD type IIa. A trend was found between fast activity and PNH, rhythmic sharp activity and FCD type I, repetitive fast spikes bursts and FCD type IIb, slow burst and HS. In 62 of the 102 patients, a complete surgical resection of the SEEG-SOZ was performed, and in 12 patients a partial resection was carried out to preserve eloquent areas. In 18 patients (15 with PNH) the SEEG-SOZ was thermo-coagulated. Seizure freedom was achieved in 58% of surgically treated patients and in 72% of those treated with thermocoagulation (mean ± SD follow-up 5.9 ± 2.3 years). Seizure freedom after surgery was achieved in 84% of the patients with PMG, FCD I, IIa and IIb presenting with characteristic SEEG-SOZ patterns. With the exception of FCD type II, interictal activity was not sufficient to identify SEEG-SOZ boundaries. *Conclusion*: The study demonstrates that specific histopathologies correlate with particular neurophysiological patterns, reflecting lesion-specific seizure patterns in focal epilepsies.

1. Introduction

Surgery is a reliable treatment option [1–6] for drug-resistant focal epilepsies associated with cortical structural lesions [7,8]. When no lesion is detected with high resolution magnetic resonance (MR), or when the lesion extension cannot be outlined by neuroimaging [9,10], additional intracerebral neurophysiological information is needed, in order to identify the brain area to be resected to achieve post-surgical seizure freedom [11]. Stereo-electro-encephalography (Stereo-EEG) reveals intralesional and perilesional electrical activities, which define the *Stereo-EEG identified Seizure Onset Zone* (SEEG-SOZ) and its network. [11–13] Moreover, Stereo-EEG represents a unique tool to obtain direct intracerebral recordings, which allow to localize and identify interictal and ictal activities, and to correlate these patterns with the anatomical

Abbreviations: EZ, epileptogenic zone; FCD, focal cortical dysplasia; HS, hippocampal sclerosis; IZ, irritative zone; LVFA, low-voltage fast activity; LZ, lesional zone; MR, magnetic resonance; FA, fast activity; PMG, polymicrogyria; PNH, periventricular nodular heterotopia; RFSB, Repetitive fast spikes bursts; RSA, rhythmic sharp activity; Stereo-EEG, stereo-electroencephalography; SOZ, seizure onset zone; SEEG-SOZ, stereo-EEG identified seizure onset zone; SB, Slow burst; THC, thermo-coagulation

* Corresponding author at: Epilepsy Unit, Fondazione IRCCS Istituto Neurologico Carlo Besta, Via Celoria 11, 20133 Milan, Italy.
E-mail addresses: roberta.digiacomo@istituto-besta.it (R. Di Giacomo), ruribe@med.puc.cl (R. Uribe-San-Martin), roberto.mai@ospedaleniguarda.it (R. Mai), stefano.francione@ospedaleniguarda.it (S. Francione), lino.nobili@ospedaleniguarda.it (L. Nobili), ivana.sartori@ospedaleniguarda.it (I. Sartori), francesca.gozzo@ospedaleniguarda.it (F. Gozzo), veronica.pelliccia@ospedaleniguarda.it (V. Pelliccia), onofrj@unich.it (M. Onofrj), giorgio.lorusso@ospedaleniguarda.it (G. Lo Russo), marco.decurtis@istituto-besta.it (M. de Curtis), laura.tassi@ospedaleniguarda.it (L. Tassi).
[1] These authors equally contributed to this work.

https://doi.org/10.1016/j.seizure.2019.10.001
Received 27 March 2019; Received in revised form 24 September 2019; Accepted 1 October 2019

lesions [14]. Hippocampal sclerosis (HS) and malformations of cortical development are recognized in about 90% of surgery patients [15]. In a few recent studies these lesions were found to be associated with peculiar Stereo-EEG interictal and ictal patterns [16–18]. Bragin and his coworkers observed in a rat model of temporal lobe epilepsy both *low-voltage fast activity* (LVFA) and *hypersynchronous* electrographic seizure-onset patterns. These activities resulted similar to those observed in patients with HS: *hypersynchronous* ictal onset originated predominantly in hippocampus, whereas LVFA ictal onset more often involved extra-hippocampal structures [19].

In 2002, we described specific intracerebral ictal Stereo-EEG patterns in focal cortical dysplasia (FCD) type II, characterized by repetitive fast spikes (defined as "*brushes*"), followed by slow waves and by LVFA [20]. More recently, six seizure-onset patterns were identified using visual and time-frequency analysis in FCD and neurodevelopmental tumors [21,22]: (i) LVFA, (ii) *preictal spiking* followed by LVFA, (iii) *burst of polyspikes* followed by LVFA, (iv) *slow wave/DC shift* followed by LVFA; (v) *theta/alpha sharp waves*, and (vi) rhythmic spikes/spike-waves. In these studies, the presence of LVFA seizure onset pattern was associated to better prognosis [21,22]. Singh and her colleagues reviewed 21 articles and reported that (i) *low frequency high amplitude repetitive spiking* is the most frequently seizure onset pattern associated with mesial temporal lobe epilepsy, bearing good post-surgical outcome, (ii) LVFA is the most commonly described pattern in neocortical epilepsy associated with good surgical outcome and (iii) *delta activity* is infrequently reported and is mostly described as a propagated seizure pattern [23].

A recent computer-assisted study identified two main focal Stereo-EEG seizure patterns: (i) *P-type*, typical of neocortex, characterized by a sharp-onset/sharp-offset transient superimposed on LVFA and (ii) *L-type* seizure pattern which involves mesial temporal structures, characterized by LVFA superimposed on a slow potential shift [24].

Only a minority of the above-mentioned studies observed correlation between Stereo-EEG patterns and underlying pathologies. Our study aims to assess such correlation on a retrospective cohort of patients with drug-resistant epilepsy, who underwent Stereo-EEG monitoring during pre-surgical work-up. The relationship between each correlated pattern-histopathology pair and the surgical outcome is also analyzed.

2. Materials and methods

2.1. Patients

Patients were retrospectively selected from the clinical database collected at the *Claudio Munari* Epilepsy Surgery Centre of the Niguarda Hospital in Milan, over an 11-year historical extension (2005–2016). Database collection for investigational purposes was approved by the local Ethics Committee and informed consent was signed by all patients. We selected patients who met all the following inclusion criteria: a) patients with drug-resistant epilepsy requiring mandatory invasive Stereo-EEG; b) patients with histopathological and/or imaging features unequivocally diagnosed with specific lesion; c) patients undergoing long-term Stereo-EEG recordings during the pre-surgical work-up with at least one spontaneous seizure recorded and at least one electrode positioned into the anatomical lesion; d) post-surgical seizure outcome follow-up (Engel's scale [25]) at least one year after surgery, e) patients submitted to either surgery or radiofrequency Stereo-EEG-guided thermocoagulation (THC) for therapeutic reasons. Informed consent for a comprehensive pre-surgical evaluation was obtained from the patients or their caregivers. Clinical data are summarized in Table 1.

2.2. Magnetic resonance imaging

MR imaging was performed using Achieva 1.5 T magnet (Philips Healthcare, Best, The Netherlands). The protocol included axial and coronal T1- and T2-weighted images, with fluid-attenuated inversion recovery (FLAIR) sequences and a volumetric T1-weighted sequence to allow 3D-volume and surface reconstructions [9]. Intravenous contrast was injected only in case of uncertain diagnosis. The nature, site and extension of presumed lesion were assessed in multidisciplinary meetings with neurologists, neurophysiologists, neuroradiologists and neurosurgeons.

Table 1
Clinical data and ictal Stereo-EEG findings.

	PMG	PNH	FCD I	FCD IIa	FCD IIb	HS
Number	15	19	17	20	19	12
Age at surgery (mean±SD, years) *	27.9 ± 12.1	34.2 ± 12.2[a]	23.2 ± 12.2	22.5 ± 11.6[a]	23.9 ± 10.6	29.2 ± 8.5
Gender (F/M)	8/7	10/9	6/11	10/10	13/6	8/4
Epilepsy duration (mean±SD, years) *	19.1 ± 12.2	18.0 ± 11.3	14.2 ± 10.1	15.3 ± 10.7	16.4 ±10.2	24.8 ± 9.3
Engel's class						
- Ia	6	15	9	14	13	5
- Ib	0	0	0	2	3	0
- Ic	3	1	1	0	0	3
- Id	1	0	0	1	2	3
- II	2	1	4	1	0	0
- III	2	1	2	2	1	1
- IV	1	1	1	0	0	0
Anatomical SEEG-SOZ location						
- Frontal	8	3	5	16[b]	13	0
- Temporal	8	15	10	1	2	12[c]
- Parietal	6	5	3	2	5	0
- Occipital	2	4	4	0	3	0
- Insular	6	0	2	6	5	0
Complete SEEG-SOZ resection	6/12	2/4	12/17	16/20	17/19	8/12
Follow up (mean±SD) *	5.5 ± 3.0	4.4 ± 2.7	6.1 ± 3.2	6.4 ± 3.3	7.1 ± 2.6	6.3 ± 2.5
range years	1.4-10.8	1.4-10	1.8-11	1.8-11.5	2-11.3	1.8-10.4
SEEG-SOZ patterns						
- LVFA	14[d]	10	7	1	3	3
- FA	0	8	2	1	5	4
- RSA	1	0	4	0	0	2
- RFSB	0	1	1	17[e]	11	0
- SB	0	0	3	1	0	3
Duration (mean±SD, seconds)*	48.7 ± 60.1[f]	79.5 ± 81.6	71.2 ± 48.7	47.9 ± 75.1[g]	31.8 ± 24.2[h]	107.4 ± 38.2[f,g,h]

PMG: Polymicrogyria, PNH: Periventricular Nodular Heterotopia, FCD: Focal Cortical Dysplasia, HS: Hippocampal Sclerosis. *Data in media (X) and standard deviation (SD). Variable age: [a]PNH was older than FCD IIa, $p < 0.05$. Anatomical SEEG-SOZ: [b]FCD IIa were more frequent in frontal lobe, $p < 0.0001$. [c]HS only was found in temporal lobe, $p < 0.0001$. SEEG-SOZ patterns: [d]PMG presented more frequently *LVFA*, $p < 0.0001$. [e]FCD IIa presented more frequently *RFSB*, $p < 0.0001$. Duration: [f]HS presented a longer duration with respect to PMG, $p < 0.01$; [g]FCD IIa, $p < 0.001$ and [h]FCD IIb, $p < 0.001$.

2.3. Stereo-EEG procedure

Stereo-EEG was tailored to the anatomical and electro-clinical features of the patients, as described by Cardinale et al. [26] Multi-lead electrodes with 5–18 recording sites (2 mm in length and 1.5 mm apart; Dixi; Besançon, France) were surgically inserted intracerebrally, a few weeks after stereo-arteriography, according to the standard protocol [26]. The co-registered T1-weighted 3D MR images enable an accurate localization of the electrodes. Stereo-EEG recordings synchronized to video-monitoring were obtained over 5–20 days. During the work-up, electrical bipolar stimulations of adjacent contacts were carried out at low-frequency (1 Hz, pulse width 1–3 msec, 15–30 sec) and high-

frequency (50 Hz, pulse width 1 msec, 5 s) to map functionally eloquent regions and to reproduce ictal manifestations (IRES 600 CH electrical stimulator, Micromed or OSIRIS NeuroStimulator, Inomed). Evoked potentials were also performed to identify physiological functions in specific regions of interest. When the SEEG-SOZ was clear-cut and univocally located, SEEG guided radiofrequency THC was performed, according to the method described by Guénot [27]. This procedure is extremely successful in malformations such as periventricular nodular heterotopia (PNH) [28]. Finally, when at least one seizure was recorded and the functional mapping was obtained, the electrodes were removed.

2.4. Stereo-EEG analysis

For Stereo-EEG video-monitoring, a Nihon Kohden System with 192 channels recorded at 1000 Hz sampling rate was used. Wake and sleep recordings were examined by two neurologists (LT, VP) to define the Lesional Zone (LZ, cortical area in which background activity is altered and slow waves are predominant), the Irritative Zone (IZ, site of spiking activity). In this manuscript, we defined as 'Stereo-EEG identified Seizure Onset Zone' (SEEG-SOZ) the area of cortex which is indispensable for the generation of epileptic seizures based on Stereo-EEG analysis. The seizure onset zone (SOZ) can also be defined "the site of the beginning of the epileptic seizures and of the primary organization" of the ictal discharge. [29–31] This definition is different from the post-hoc and operational designation of the ZE as the cortical tissue to be removed in order to treat the patient [32].

We reviewed wake and sleep interictal and ictal recordings to delineate the LZ, the IZ and the SEEG-SOZ [29,33]. The identification of the LZ, IZ and SEEG-SOZ boundaries were consistent among different reviewers; possible discrepancies were solved after open discussion.

2.4.1. Interictal activity and the SEEG-SOZ

We calculated the percentage of leads involved both in seizure onset (SEEG-SOZ) and in LZ/IZ during wakefulness, in comparison to the total involved wake leads:

$$\frac{n^\circ \textit{ leads (SEEG-SOZ) involved in wake LZ (or IZ)}}{\textit{TOT } n^\circ \textit{ leads involved in wake LZ (or IZ)}} * 100$$

We also calculated the percentage of leads involved in seizure onset and LZ/IZ during sleep, with respect to the total of leads involved in sleep LZ/IZ:

$$\frac{n^\circ \textit{ leads (SEEG-SOZ) involved in sleep LZ (or IZ)}}{\textit{TOT } n^\circ \textit{ leads involved in sleep LZ (or IZ)}} * 100$$

In addition, we calculated the percentage of leads involved both in seizure onset and in wake LZ or IZ, with respect to all leads included in seizure onset:

$$\frac{n^\circ \textit{ leads (SEEG-SOZ) involved in wake LZ (or IZ)}}{\textit{TOT } n^\circ \textit{ leads (SEEG-SOZ)}} * 100$$

Finally, we calculated the same percentages in sleep:

$$\frac{n^\circ \textit{ leads (SEEG-SOZ) involved in sleep LZ (or IZ)}}{\textit{TOT } n^\circ \textit{ leads (SEEG-SOZ)}} * 100$$

Table 2.A summarizes the results.

2.4.2. Post-ictal suppression and seizure onset zone

We evaluated the percentage of leads involved both in seizure onset and in postictal suppression, with respect to the total recording leads. Electrical seizure termination was characterized by focal disorganized or depressed background activity, without paroxysmal features [34] usually associated to slow waves. The percentage of leads involved both in seizure onset and in post-ictal suppression was calculated with respect to the total leads with suppression:

Table 2
A: Concordance between the percentage of SEEG-SOZ leads involved in either LZs or IZs (LZ: slow waves with disrupted background activity, IZ: spiking activity) during wake and sleep, in patients with different lesions. **B**: Percentage of SEEG-SOZ leads involved in postictal suppression in patients with different lesions.

A

	PMG	PNH	FCD I	FCD IIa	FCD IIb	HS
Wake LZ	28±28	12±22[b]	38±30	79±28	78±28	35±27[d]
Sleep LZ	24±20[a]	9±21[c]	32±28	82±26	74±34	39±27[e]
Wake IZ	35±29	58±35[b]	48±33	87±19	83±22	80±27[d]
Sleep IZ	45±32[a]	58±33[c]	45±31	87±23	80±27	79±32[e]
Mean±SD	33±28[fg]	34±37[fg]	41±30[fg]	**84±24[f]**	**79±28[g]**	58±35[f]

B

	PMG	PNH	FCD I	FCD IIa	FCD IIb	HS
(%) Mean±SD	64±31	59±41	53±32	86±25[a]	79±27	40±41[h]

PMG: Polymicrogyria, PNH: Periventricular Nodular Heterotopia, FCD: Focal Cortical Dysplasia, HS: Hippocampal Sclerosis. [a]p: 0.029, [b]p < 0.0001, [c]p < 0.0001, [d]p: 0.001, [e]p: 0.003, [f]p: 0.001, [g]p: 0.001, [h]p: 0.01.

$$\frac{n^\circ \textit{ leads (SEEG-SOZ) with/post-ictal suppression}}{\textit{TOT } n^\circ \textit{ leads with/post-ictal suppression}} * 100$$

We also assessed the percentage of leads involved both in seizure onset and in post-ictal suppression, with respect to all leads included in seizure onset:

$$\frac{n^\circ \textit{ leads (SEEG-SOZ) with/post-ictal suppression}}{\textit{TOT } n^\circ \textit{ leads (SEEG-SOZ)}} * 100$$

These calculations showed the percentage of leads that presented both ictal onset pattern and post-ictal suppression. Table 2.B summarizes these results.

2.5. Histopathology procedures

The surgical specimens were fixed in 10% neutral buffered formalin and were paraffin-embedded. Sections (4-10 μm) were stained using haematoxylin and eosin, thionin, Kluver-Barrera and Bielschowsky techniques. Routine immunocytochemical investigations were also performed using anti-glial fibrillary acid protein (GFAP: Roche Diagnostics, Mannheim, Germany or Chemicon International, Temecula, CA, U.S.A.), anti-neurofilament (2F11 monoclonal, DAKO, Denmark; SMI311R, Covance, San Diego, CA, U.S.A.) and neuron-specific nuclear protein (NeuN; Chemicon).

2.6. Statistical analysis

Because of the non-normal distribution of the data, differences in quantitative variables between the groups were established using two tailed Kruskal-Wallis and Dunn´s multiple comparison tests. Differences were considered significant at $p < 0.05$. For qualitative variables, the Fisher exact test and Bonferroni correction for multiple comparison were used. For results between ictal pattern and histology, a Receiver Operating Characteristic (ROC) curve was created, with their respective Area Under the Curve (AUC). Sensibility, specificity, positive predictive value and negative predictive value were also calculated. Odds Ratio (OR) and 95% confidence interval (CI) were calculated with binomial logistic regression, applied in order to identify confounding interactions among every ictal pattern, histopathologies and lobes involved. Kaplan-Meier survival curves were used to compare the probability of remaining in Engel class Ia, for patients who underwent complete and incomplete SEEG-SOZ resections.

The results were reported using mean ± standard deviation (SD),

median, range and percentages. For statistical analysis IBM SPSS Statistics 21 was used and GraphPad 5 for graphics.

3. Results

Of the 102 patients included in the study, 55 were females (53,9%) and 47 males (46.1%), with mean ± SD age of 26.6 ± 12 years at surgical treatment and epilepsy duration of 17.5 ± 10.9 years. Structural lesions neuroradiologically identified and/or demonstrated after neuropathological evaluation were: 15 PMGs, 19 PNHs, 17 FCDs type I, 20 FCDs type IIa, 19 FCDs type IIb and 12 HS. Mean ± SD post-surgical follow-up was 5.9 ± 2.3 years (range 1.4–11.5 years). Postsurgical seizure outcome was evaluated according to the scale developed by Engel: [25] 62 patients (68%) were in Engel's class Ia, 5 in class Ib (4.9%), 8 in Ic (7.8%), 7 in Id (6.9%), 8 in class II (7.8%), 9 in class III (8.8%) and 3 in class IV (2.9%). Table 1 summarizes patients' clinical characteristics grouped by histopathology.

We reviewed wake and sleep interictal recordings, as described in the Methods and as previously defined [30,33]. For each neuropathological entity, we reported the percentage of leads involved in LZ and/or IZ, with respect to the total SEEG-SOZ leads. We assessed the association between the location of interictal abnormalities with respect to the SEEG-SOZ in different patient sub-groups. For all measurements, no significant differences were observed between wake and sleep conditions (Table 2A).

The study of the association between different SEEG-SOZ patterns and the underlying pathologies revealed 5 different seizure onset patterns (see Fig. 1]): 1) *Low-voltage fast activity* (*LVFA*; < 10 μV) characterized by > 100 Hz fast activity and initial amplitude that starts abruptly and may be accompanied by DC shift or a slow-wave [13,35–37]. 2) *Fast activity* (*FA*) between 13 and 100 Hz with medium voltage amplitude, it is usually non-tonic activity, accompanied by DC shift or interictal spikes. 3) *Rhythmic sharp activity* (*RSA)* that featured either high-voltage sharply-contoured rhythmic activity in the *alpha-theta* range [35,36,38] or spindle-like elements. 4) *Repetitive fast spikes bursts* (*RFSB*), similar to previously defined *brushes* [39], characterized by brief sequences of low-amplitude high frequency polyspikes, often preceded by repetitive spikes or spike and wave complex, and followed by LVFA or FA. 5) *Slow burst* (*SB*) of repetitive high-voltage spikes or spike and wave complex, typically recurring at a frequency of 0.5–4 Hz [37].

3.1. Interictal abnormalities and the SEEG-SOZ

Signal patterns observed during the interictal periods (LZ and IZ) were described in the Methods. In most histopathological groups, a weak correlation was observed between interictal abnormalities (LZ and IZ) and SEEG-SOZ, with the exception of FCD type IIa and IIb (Table 2.A). The active leads for interictal abnormalities and SEEG-SOZ were concordant on average in 84±24% and 79±28% for FCD IIa and IIb, respectively. Concordance was not significant (Table 2.A) for all other lesions. The dependence between IZ and SEEG-SOZ was higher than the one between LZ and SEEG-SOZ, in particular for PNH and HS. We did not find significant differences between wake and sleep states.

Specific interictal activities in the LZ were considered to be pathognomonic of PNH: intranodular background rhythms consisted in flattening periods mixed with low voltage low frequency activities, with frequent angled high voltage spikes, asynchronous among different nodules and synchronous with the overlying cortex in the majority of cases [40]. This activity was not related with a specific lobar location of the nodules. Lesion-specific interictal activity was observed also in FCD type II; it was characterized by the total absence of background activity and by repetitive, high amplitude and fast spikes, followed by high amplitude slow waves, similar to ictal *RFSB*, mixed with relatively flat inter-bursts periods. This activity, defined as *brushes,* recurred pseudo-periodically [20,39]. Different parts of the FCD exhibited *brushes* with variable frequency and synchronicity in the same patient.

3.2. Association between SEEG-SOZ patterns and histopathologies

The revision of SEEG-SOZ patterns demonstrated correlations with specific histopathologies. We found a statistically significant association between *LVFA* and PMG, as well as between *RFSB* pattern and the presence of FCD type IIa, with AUC of 85% and 83% respectively in the ROC curves ($p < 0.0001$, Table 3). A trend was also observed between *RFSB* and FCD type IIb, *FA* with PNH, *RSA* with FCD type I and *SB* with HS, although these associations did not endure the more restrictive Bonferroni correction for multiple comparisons. Table 3 shows AUC values, sensitivity, specificity and positive predictive values and negative predictive values; Fig. 2 highlights ictal patterns distribution among histopathologies.

SEEG-SOZ pattern analysis in HS, observed according to ILAE classification [35], did not show specific patterns in the groups of patients

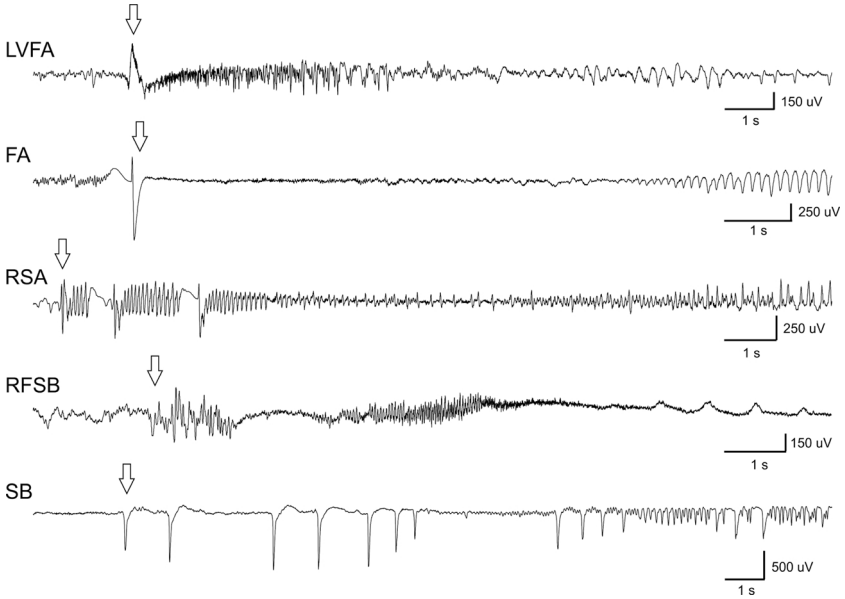

Fig. 1. Seizure Onset Zone Stereo-EEG patterns. LVFA: *Low-voltage fast activity* with slow DC shift; FA: *Fast activity;* RSA: *Rhythmic sharp activity;* RFSB: *Repetitive fast spikes bursts;* SB: *Slow burst* of polyspikes. Seizure onset is marked by the arrow. Bipolar montage.

Table 3
Histology and SEEG-SOZ patterns analysis.

Histology / SEEG-SOZ Patterns	AUC[a]	Sensibility	Specificity	PPV	NPV	p Value[b]
PMG / *LVFA*	83%	93%	72%	37%	98%	< 0.0001
PNH / *FA*	64%	42%	86%	40%	87%	0.011
FCD I / *RSA*	60%	24%	97%	57%	86%	0.014
FCD IIa / *RFSB*	85%	85%	84%	57%	96%	< 0.0001
FCD IIb / *RFSB*	68%	58%	77%	37%	89%	0.005
HS / *SB*	60%	25%	96%	43%	91%	0.034

PMG: Polymicrogyria. PNH: Periventricular Nodular Heterotopia. FCD: Focal Cortical Dysplasia. HS: Hippocampal Sclerosis. *LVFA*: Low-Voltage Fast Activity. *FA*: Fast Activity. *RSA*: Rhythmic Sharp Activity. *SB*: Burst of high-amplitude polyspikes or spike and wave complex. AUC: Area Under Curve. PPV: Positive Predictive Value, NPV: Negative Predictive Value. [a]AUC using Receiver Operating Characteristic curve; [b]p value obtained using Fisher Exact Test. We considered statistically significant the p values obtained with Fisher Exact Test and Bonferroni correction for multiple comparison with a factor of 30 (six histopathologies by five ictal patterns), corresponding to a significative adjusted alpha of $p < 0.00167$.

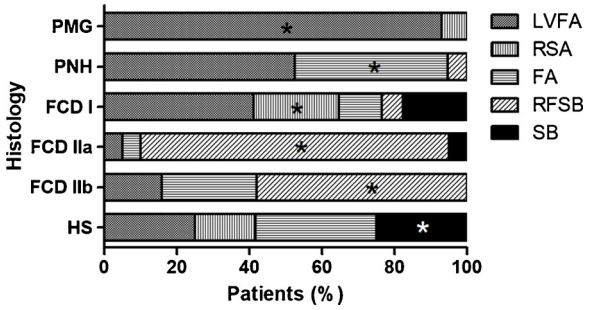

Fig. 2. SEEG-SOZ pattern grouping with respect to their histopathology. PMG: Polymicrogyria. PNH: Periventricular Nodular Heterotopia. FCD: Focal Cortical Dysplasia. HS: Hippocampal Sclerosis. *LVFA*: Low-Voltage Fast Activity. *FA*: Fast Activity. *RSA*: Rhythmic Sharp Activity. *SB*: slow burst of high-amplitude polyspikes or spike and wave complex. *p value (Table 3) obtained using Fisher Exact Test. We considered statistically significant the p values obtained with Fisher Exact Test and Bonferroni correction for multiple comparison with a factor of 30 (6 histopathologies by 5 ictal patterns), corresponding to a significative adjusted alpha of $p < 0.00167$.

with normal hippocampal volumes and with hippocampal atrophy ($p = 0.74$).

Subsequently, we evaluated the influence of the lesion localization on ictal pattern and histopathology. Sixty-four patients presented mono-lobar seizure onset; for the multilobar seizures we consider every lobe involved. Different seizure patterns were observed in all lobes, but *RSA* was never found in the frontal lobe and *SB* was never observed in the insula and in occipital or parietal lobes. *RFSB* were more frequent in the frontal lobe (Table 4, $p < 0.0001$). However, when performing a binary logistic regression using *RFSB* pattern as dependent variable, and both FCD type IIa histology and lobar location as independent co-variables, an association was confirmed despite localization (OR: 18.2, 95% CI: 3.8–87.4, p: 0.0001, Table 4).

3.3. Singular characteristics of SEEG-SOZ patterns among histopathologies

Particular features of ictal onset, spread, post ictal suppression and ictal duration during seizures were found among different histopathologies.

3.3.1. Ictal onset

Ictal *LVFA* pattern was accompanied with a DC-shift in patients with PMG (12/14) and PNH (10/10); only one PNH patient presented *FA* with DC-shift. However, none of the FCD type II patients with *LVFA* (1/20 FCD type IIa and 3/19 FCD type IIb) showed DC-shift. Finally, FCD type I was the only histopathology in which we identified all types of ictal patterns.

Table 4
Anatomical location and SEEG-SOZ patterns.

	Frontal (n° pts)	Temporal (n° pts)	Parietal (n° pts)	Occipital (n° pts)	Insula (n° pts)
LVFA	14	22	10	6	10
RSA	0	6	1	2	1
FA	5	12	5	4	1
RFSB	24[a]	3	5	1	7
SB	2	5	0	0	0

Anatomical SEEG-SOZ location and *RFSB* pattern*

	OR	95% CI		p value
FCD type IIa	18.2	3.8	87.4	0.0001
Frontal	4.2	0.6	28.0	0.138
Temporal	0.3	0.1	2.0	0.203
Parietal	2.7	0.5	15.0	0.258
Occipital	0.5	0.1	7.2	0.630
Insula	0.6	0.1	2.6	0.519

LVFA: Low-Voltage Fast Activity, *FA*: Fast Activity, *RSA*: Rhythmic Sharp Activity at < 13 Hz, *SB*: Burst of high-amplitude polyspikes or spike and wave complex. [a]Frontal lobe presented more frequently *RFSB*, $p < 0.0001$. We considered statistically significant the p values obtained with Fisher Exact Test and Bonferroni correction for multiple comparison with a factor of 25 (5 lobes by 5 ictal patterns), corresponding to a significative adjusted alpha of $p < 0.002$.
*The multivariate analysis with binary logistic regression using *RFSB* pattern as dependent variable, FCD type IIa as characteristic histology and each brain lobe as independent co-variables, revealed an association between *RFSB* and FCD type IIa, despite localization.

3.3.2. Spread

In 12 of 17 FCD type IIa (71%) *RFSB* was followed by *LVFA* and in 5 patients by *FA*. In FCD type IIb patients presenting *RFSB* as ictal onset pattern, in 6 cases *RFSB* was followed by *LVFA* and in 3 cases by *FA*, while in 2 cases *RFSB* was not followed by fast activity. In FCD type IIb, we also found isolated *LVFA* in 3 out of 19 patients. In FCD group, *FA* with increasing interictal spikes prevailed (FCD type I 1/2, FCD type IIa 1/1, FCD type IIb 5/5). In PNH and FCD type I, we rarely observed *RFSB* without *LVFA*. In FCD type I and in HS, the ictal discharge rapidly became spatially diffused. In HS, peculiar high amplitude positive spikes at a frequency of 1–2 Hz were found, and discharge propagation across leads occurred slowly and diffusely over several seconds.

3.3.3. Post ictal suppression

In FCD type IIa and IIb, postictal suppression remains localized and concordant with SEEG-SOZ (86 ± 25% and 79 ± 27%, respectively). In HS, a widespread postictal suppression was observed, with a concordance between suppression zone and the SEEG-SOZ of 40 ± 41% cases (Table 2.B).

3.3.4. Duration

HS presented with a longer seizure duration (107.4 ± 38.2 s) with respect to other histopathologies,[24] with statistically significant differences compared to PMG (48.7 ± 60.1 s, $p < 0.01$), FCD IIa (47.9 ± 75 s, $p < 0.001$) and FCD IIb (31.8 ± 24.2 s, $p < 0.001$) (Table 1).

3.4. Prognostic factors

Of the 102 patients analyzed, 84 had surgery and in 18 patients THC of the SEEG-SOZ leads was performed (15 of them with PNH). The percentage of seizure-free patients (Engel class Ia) by the end of the follow-up were 58.3% (49/84) in the surgical and 72% (13/18) in THC

groups. Complete SEEG-SOZ surgical resection was achieved in 62 of 84 patients and partial SEEG-SOZ resection was intentionally performed in the rest of the cases, to preserve eloquent areas (sensory, language and motor functions). As expected [22,23,30,33], complete resection of the SEEG-SOZ was a protective prognostic factor for achieving seizure freedom after the surgery ($p < 0.0001$ Log-rank test).

When analyzing the post-surgical seizure outcome in patients with complete SEEG-SOZ resection, we found differences in post-surgical prognosis for each histopathology with specific SEEG-SOZ patterns. Six out of seven PMG patients (85.7%) with *LVFA* were seizure free. In PNH no differences in post-surgical outcome were observed between *FA* and other patterns. In FCD type I, all patients with *RSA* (4) and 62.5% (5/8) with other patterns reached seizure free status. A high rate of seizure freedom was observed among patients with FCD type IIa (87.5%, 14/16), 12 of which presented with typical *RFSB* pattern. However, in FCD type IIb, seizure freedom was achieved in 66.7% (6/9) of patients having typical *RFSB* pattern compared to 87.5% (7/8) of those having other patterns. Five out of 8 patients with HS (62.5%) achieved seizure freedom and only 1 HS patient had *SB* ictal pattern.

4. Discussion

We describe the ictal and interictal Stereo-EEG patterns of over a hundred patients with drug-resistant epilepsy due to PMG, PNH, FCD type I, IIa, IIb and HS demonstrated by MRI and/or histopathological findings. As in previous studies [13,16,22,39], five prevalent SEEG-SOZ patterns were observed. Considering the activity recorded at seizure onset in the leads with a strict relationship with the lesion, a statistically significant dependency was found between the presence of *LVFA* and PMG, and between *RFSB* and FCD type IIa. A correlation trend was observed between *RFSB* and FCD type IIb, *FA* and PNH, *RSA* and FCD type I, *SB* and HS. When assessing post-surgical prognosis, complete SEEG-SOZ resection was a predictive factor for seizure freedom. This is not unexpected and has been previously reported [22,25,32,41]. Most patients with PMG, FCD type I, IIa and IIb presenting pathognomonic ictal patterns (*LVFA, RSA* and *RFSB*, respectively) achieved seizure freedom after surgery with significant frequency. These findings support the hypothesis that different histopathologies have a peculiar neurophysiological pattern, although not a unique one. The data also demonstrate that resection/THC of lesions with pathology-specific ictal patterns yield the best post-treatment seizure outcome.

In our study, most seizure onset patterns show fast activity, frequently associated with DC-shift. Only two infrequent patterns, *RSA* and *SB*, exhibited *alpha* or lower frequencies band components, 10 of them recorded into the temporal lobe. Furthermore, *LVFA* was the only seizure onset pattern occurring in all histologies [16]. In line with previous studies [23], we confirmed that fast activities were mostly associated to the SEEG-SOZ, while slower patterns identified areas of secondary propagation. Ictal fast activities as biomarkers of epileptogenicity were found in all histopathologies, with the highest frequency recorded in PMG [16,42–44]. Scalp EEG *FA* at seizure onset have also shown good prognostic surgical outcomes in patients with frontal lobe or non-lesional epilepsy [45].

The correct spatial identification of the SEEG-SOZ is critical to achieve complete resection, which is the most important prognostic factor for seizure-free status after surgery [21,43,46,47]. In line with previous observations [16], we confirmed that the lobar location of the SEEG-SOZ did not impact on seizure patterns, which was mainly influenced by the underlying histopathology. Previous studies with smaller sample sizes, showed an association between *LVFA* and PMG, *RFSB* with FCD [39], and *SB* with HS [48].

According to Spanedda's observations [35], the onset pattern in HS is correlated with the severity of hippocampal atrophy: high frequencies (> 13 Hz) were predominant in the group with normal volumes hippocampi, whereas slow frequencies were more represented in patients with hippocampal atrophy. In our study, the pattern of seizure onset was not significantly related to any specific ILAE hippocampal sclerosis subtype.

The average duration of the discharges was different among the histologies: HS displayed longest seizure duration, while FCD type IIb shows the shortest seizure duration. de Curtis and his coworkers suggested that interictal events are sustained by cellular and pharmacological mechanisms which change according to the site of generation. They also suggested that interictal epileptiform discharges may control brain hyper-excitability within the epileptic network and protect the cortical region against seizure entrainment, as supported by the prolonged duration of the seizures in temporal lobe epilepsy [49]. These findings were recently confirmed by a Stereo-EEG analysis of seizure patterns in a large population of patients with focal drug-resistant epilepsy [24]; in this study seizure that involved mesial temporal regions showed longer duration in comparison to those observed in neocortical regions. Our findings indicated that electrophysiological behavior across histologies was heterogeneous in terms of both seizure onset pattern and interictal characteristics, suggesting a need for further studies about primary epileptogenic mechanisms.

Finally, our study contributes to the current debate on the relevance of ictal and interictal recordings for the identification of the SEEG-SOZ. Interictal information in our patient cohort was insufficient to clearly locate the SEEG-SOZ. FCD type II, in particular IIa, represented the only type of lesion in which interictal abnormalities could lead to define the SEEG-SOZ with great accuracy [20,39]. Interestingly, we noted that the occurrence of *RFSB* was not strictly associated to FCD with balloon cells (type IIb) [39], and represented a distinctive pattern also in FCD type IIa.

There are several limitations to the present study. The most important are the retrospective approach, the small sample size and the inclusion of very challenging pre-surgical patients. Prospective studies will be necessary in order to validate the reliability and the relevance in clinical practice of our results.

In conclusion, this paper demonstrates that the tridimensional spatial delineation of the SEEG-SOZ, based on ictal and interictal Stereo EEG features, can be exploited to draw a relationship with the underlying lesion type. The specific histopathological substrates generate lesion-specific electrical fingerprint, which may help to clarify patient prognosis and could contribute to guide and to improve a successful strategy for surgical resection and THC treatments.

Author's contribution

L.T., R.D.G., V.P., R.M., S.F., F.G., L.N., I.S. and R.U.S.M contributes to conception and design of study, L.T. and V.P. reviewed recordings, R.D.G. performed data collection, R.U.S.M. and R.D.G analyzed the data, L.T., V.P., R.M., S.F., F.G., L.N., I.S., G.L.R., M.O. supervised the project, R.D.G., R.U.S.M. M.d.C. and L.T. wrote the manuscript, L.T., G.L.R. M.O. and M.d.C. controlled the manuscript.

Declaration of Competing Interest

None.

Acknowledgements

Authors thank the *Claudio Munari* Epilepsy Surgery Centre multidisciplinary and technical team for their support in the development of this paper and Professors Ethel Ciampi, Jaime Godoy and Valerio Scacco for theirs support in English-language editing.

Thanks to Epilepsy Program of Health Ministry of Chile and Pontifical Catholic University of Chile for providing a special support to Uribe-San-Martín R. for a long stage study at the *Claudio Munari* Epilepsy Surgery Centre.

References

[1] Horsley V. Brain-surgery. BMJ 1886;2:670–5.
[2] Jackson JH. A study of convulsions. Arch Neurol 1970;22:184–8.
[3] Talairach J, Bancaud J, Bonis A, et al. Surgical therapy for frontal epilepsies. Adv Neurol 1992;57:707–32.
[4] Tassi L, Meroni A, Deleo F, et al. Temporal lobe epilepsy: neuropathological and clinical correlations in 243 surgically treated patients. Epileptic Disord 2009;11:281–92.
[5] Effectiveness and Efficiency of Surgery for Temporal Lobe Epilepsy Study Group. Wiebe S, Blume WT, Girvin JP. A randomized, controlled trial of surgery for temporal-lobe epilepsy. N Engl J Med 2001;345:311–8.
[6] Wyllie E, Comair YG, Kotagal P, et al. Seizure outcome after epilepsy surgery in children and adolescents. Ann Neurol 1998;44:740–8.
[7] Spencer DD, Spencer SS, Mattson RH, et al. Intracerebral masses in patients with intractable partial epilepsy. Neurology 1984;34:432–6.
[8] Palmini A, Gambardella A, Andermann F, et al. Intrinsic epileptogenicity of human dysplastic cortex as suggested by corticography and surgical results. Ann Neurol 1995;37:476–87.
[9] Colombo N, Tassi L, Deleo F, et al. Focal cortical dysplasia type IIa and IIb: MRI aspects in 118 cases proven by histopathology. Neuroradiology 2012;54:1065–77.
[10] Mai R, Tassi L, Cossu M, Francione S, Lo Russo G, Garbelli R, et al. A neuropathological, stereo-EEG and MRI study of subcortical band heterotopia. Neurology 2003;60:1834–8.
[11] Bartolomei F, Lagarde S, Wendling F, et al. Defining epileptogenic networks: contribution of SEEG and signal analysis. Epilepsia 2017;58:1131–47.
[12] Duchowny M, Jayakar P, Levin B. Aberrant neural circuits in malformations of cortical development and focal epilepsy. Neurology 2000;55:423–8.
[13] Lee SA, Dennis DS, Spencer SS. Intracranial EEG seizure-onset patterns in neocortical epilepsy. Epilepsia 2000;1:297–307.
[14] Munari C, Hoffmann D, Francione S, et al. Stereo-electroencephalography methodology: advantages and limits. Acta Neurol Scand 1994;152:56–67.
[15] Blümcke I. Neuropathology of focal epilepsies: a critical review. Epilepsy Behav 2009;15:34–9.
[16] Perucca P, Dubeau F, Gotman J. Intracranial electroencephalographic seizure-onset patterns: effect of underlying pathology. Brain 2014;137:183–96.
[17] Tanaka H, Khoo HM, Dubeau F, et al. Association between scalp and intracerebral electroencephalographic seizure-onset patterns: a study in different lesional pathological substrates. Epilepsia 2018;59:420–30.
[18] Chassoux F, Devaux B, Landré E, et al. Stereoelectroencephalography in focal cortical dysplasia: a 3D approach to delineating the dysplastic cortex. Brain 2000;123:1733–51.
[19] Bragin A, Engel Jr J, Wilson CL, et al. Electrophysiologic analysis of a chronic seizure model after unilateral hippocampal KA injection. Epilepsia 1999;40(September (9)):1210–21.
[20] Tassi L, Colombo N, Garbelli R, et al. Focal cortical dysplasia: neuropathological subtypes, EEG, neuroimaging and surgical outcome. Brain 2002;125:1719–32.
[21] Lagarde S, Bonini F, McGonigal A, et al. Seizure-onset patterns in focal cortical dysplasia and neurodevelopmental tumors: relationship with surgical prognosis and neuropathologic subtypes. Epilepsia 2016;57:1426–35.
[22] Lagarde S, Buzori S, Trebuchon A, et al. The repertoire of seizure onset patterns in human focal epilepsies: determinants and prognostic values. Epilepsia 2019;60(January (1)):85–95.
[23] Singh S, Sandy S, Wiebe S. Ictal onset on intracranial EEG: do we know it when we see it? State of the evidence. Epilepsia 2015;56(October (10)):1629–38.
[24] Gnatkovsky V, Pelliccia V, de Curtis M, et al. Two main focal seizure patterns revealed by intracerebral electroencephalographic biomarker analysis. Epilepsia 2019;60(January):96–106.
[25] Engel Jr J, VanNess P, Rasmussen TB, et al. Outcome with respect to epileptic seizures. In: Engel J, editor. Surgical treatment of the epilepsies. 2nd editionNew York: Raven Press; 1993. p. 609–21.
[26] Cardinale F, Cossu M, Castana L, et al. Stereoelectroencephalography: surgical methodology, safety and stereotactic application accuracy in 500 procedures. Neurosurgery 2013;72:353–66.
[27] Guénot M, Isnard J, Ryvlin P, et al. SEEG-guided RF thermocoagulation of epileptic foci: feasibility, safety, and preliminary results. Epilepsia 2004;45(November (11)):1368–74.
[28] Cossu M, Fuschillo D, Cardinale F, et al. Stereo-EEG-guided radio-frequency thermocoagulations of epileptogenic grey-matter nodular heterotopy. J Neurol Neurosurg Psychiatry 2014;85(June (6)):611–7.
[29] Talairach J, Bancaud J. Lesion, irritative zone and epileptogenic focus. Confin Neurol 1966;27(1):91–4.
[30] Munari C, Bancaud J. The role of stereo-electroencephalography (SEEG) in the evaluation of partial epileptic patients. In: Porter RJ, Morselli PL, editors. The epilepsies. London: Butterwort; 1987. p. 267–306.
[31] Kahane P, Elisabeth L, Lorella M, et al. The bancaud and Talairach View on the epileptogenic zone: a working hypothesis. Epileptic Disord 2006;8.
[32] Luders HO, editor. Testbook of epilepsy surgery. Informa he; 2006.
[33] Bancaud J. Topographic relationship between cerebral lesions and seizures discharges. In: Canger R, Angeleri F, Penry JK, editors. Advances in epileptology, XIth epilepsy International symposium. New York: Raven Press; 1980. p. 103–9.
[34] Spencer SS, Spencer DD. Implications of seizure termination location in temporal lobe epilepsy. Epilepsia 1996;37:455–8.
[35] Spanedda F, Cendes F, Gotman J. Relations between EEG seizure morphology, interhemispheric spread and mesial temporal atrophy in bitemporal epilepsy. Epilepsia 1997;38:1300–14.
[36] Wennberg R, Arruda F, Quesney LF, et al. Preeminence of extrahippocampal structures in the generation of mesial temporal seizures: evidence from human depth electrode recordings. Epilepsia 2002;43:716–26.
[37] Faught E, Ruben IK, Hurst DC. Ictal EEG wave forms from epidural electrodes predictive of seizure control after temporal lobectomy. Electroencephalogr Clin Neurophysiol 1992;83:229–35.
[38] Schiller Y, Cascino GD, Busacker NE. Characterization and comparison of local onset and remote propagated electrographic seizures recorded with intracranial electrodes. Epilepsia 1998;39:380–8.
[39] Tassi L, Garbelli R, Colombo N, et al. Electroclinical, MRI and surgical outcomes in 100 epileptic patients with type II FCD. Epileptic Disord 2012;14:257–66.
[40] Mirandola L, Mai RF, Francione S, Pelliccia V, Gozzo F, Sartori I, et al. Stereo-EEG: diagnostic and therapeutic tool for periventricular nodular heterotopia epilepsies. Epilepsia 2017;58:1962–71.
[41] Marnet D, Devaux B, Chassoux F, et al. [Surgical resection of focal cortical dysplasias in the central region]. Neurochirurgie 2008;54(May (3)):399–408.
[42] Bartolomei F, Chauvel P, Wendling F. Epileptogenicity of brain structures in human temporal lobe epilepsy: a quantified study from intracerebral EEG. Brain 2008;131:1818–30.
[43] Gnatkovsky V, de Curtis M, Pastori C, et al. Biomarkers of epileptogenic zone defined by quantified stereo-EEG analysis. Epilepsia 2014;55:296–305.
[44] Wendling F, Bartolomei F, Bellanger JJ, et al. Epileptic fast intracerebral EEG activity: evidence for spatial decorrelation at seizure onset. Brain 2003;126:1449–59.
[45] Zakaria T, Noe K, So E, et al. Scalp and intracranial EEG in medically intractable extratemporal epilepsy with normal MRI. ISRN Neurol 2012:942849.
[46] Bonini F, McGonigal A, Scavarda D, et al. Predictive factors of surgical outcome in frontal lobe epilepsy explored with stereoelectroencephalography. Neurosurgery 2018;83:217–25.
[47] Grinenko O, Li J, Mosher JC, Wang IZ, Bulacio JC, Gonzalez-Martinez J, et al. A fingerprint of the epileptogenic zone in human epilepsies. Brain 2018;141:117–31.
[48] Toussaint D, Moura M, Allouche L. Can early post-ictal activities help to better localise and lateralise the epileptogenic zone. Epilepsia 2005;46:324.
[49] de Curtis M, Jefferys JGR, Avoli M. Interictal epileptiform discharges in partial epilepsy: complex neurobiological mechanisms based on experimental and clinical evidence. In: Noebels JL, Avoli M, Rogawski MA, Olsen RW, Delgado-Escueta AV, editors. Jasper's basic mechanisms of the epilepsies. 4th ednBethesda (MD): National Center for Biotechnology Information (US); 2012.